Atmospheric tomography of a red supergiant star μ Cep

Kateryna Kravchenko[1]

S. Van Eck[1], A. Chiavassa[2], A. Jorissen[1], T. Merle[1]

[1] Institut d'Astronomie et d'Astrophysique, Université Libre de Bruxelles, Bruxelles, Belgium
[2] Université Côte d'Azur, Observatoire de la Côte d'Azur, Nice, France

UNIVERSITÉ LIBRE DE BRUXELLES

Observatoire de la CÔTE d'AZUR

Outline

- Context and goals of the present study
- Method: tomography
- Application to high-resolution spectra of a red supergiant star μ Cep
- Application to 3D radiative-hydrodynamics simulations
- Conclusions and future plans

Red supergiant stars

- Mass: 9-25 M⊙
- Teff: 3450-4100 K
- log g: between -1 and 1
- Radius: up to 1500 R⊙
- Luminosity: 20000-300000 L⊙

(Levesque 2005)

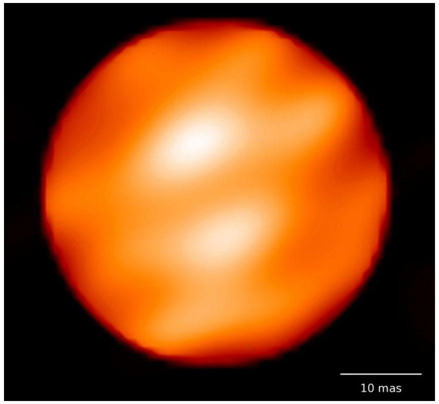

Betelgeuse H band

Haubois et al. (2009)

Antares K band

Ohnaka et al. (2017)

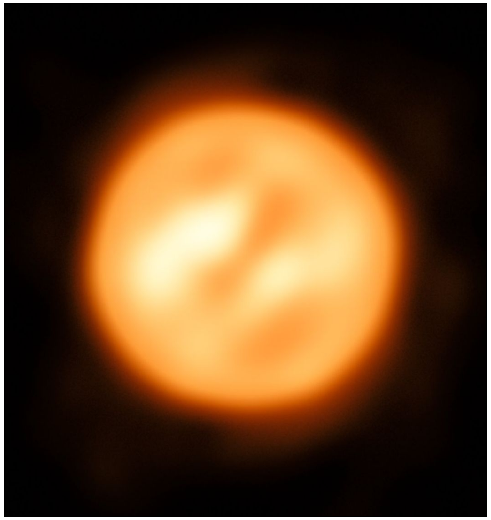

- Extended atmospheres
- Few large convective cells
- Complex velocity fields which affect spectral lines
- Irregular photometric variations

Red supergiant stars

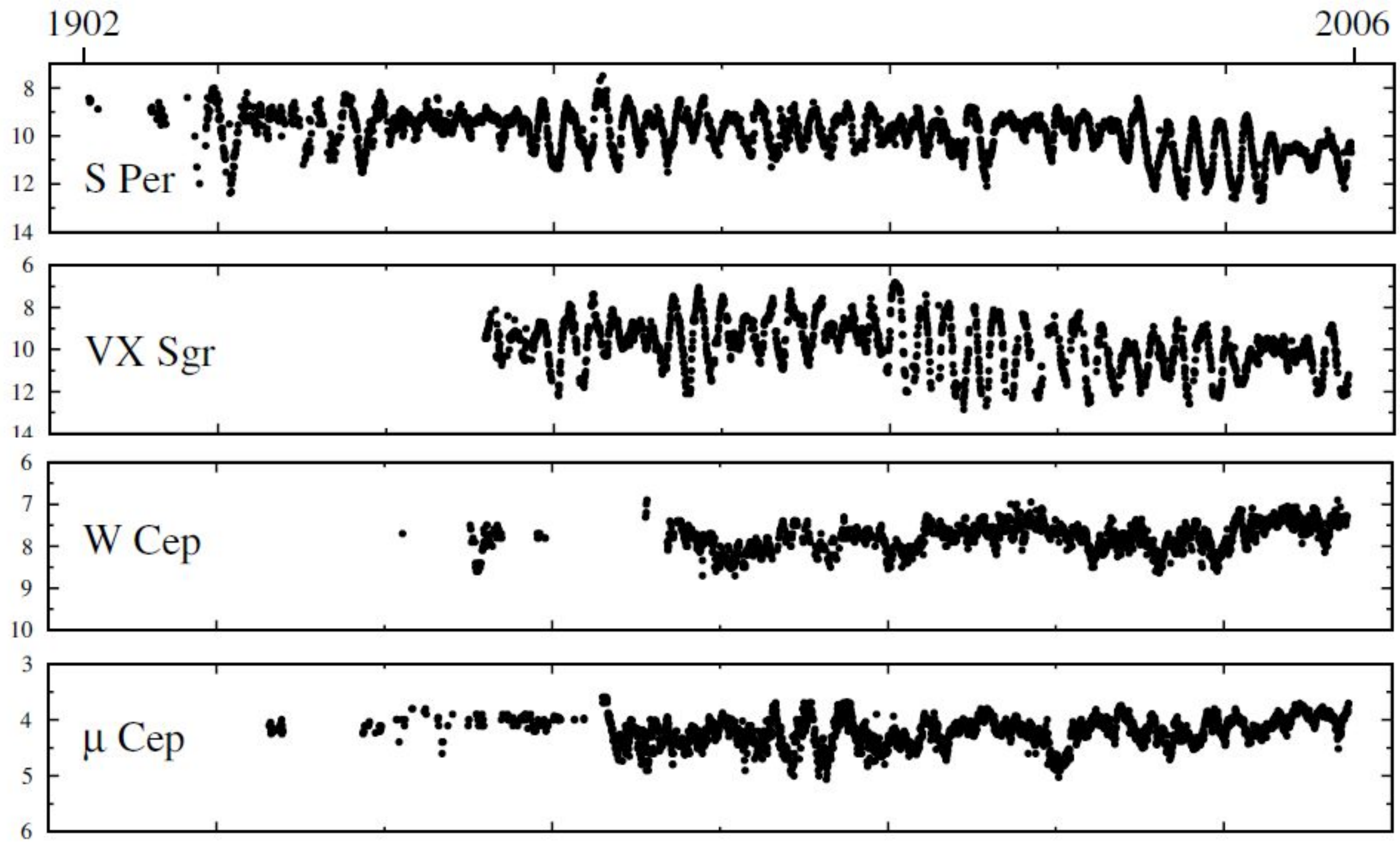

Kiss et al. (2006) ⇒ two photometric periods:

- short (few hundred days) ⇒ convection? pulsations?
- long (few thousand days) ⇒ binarity? magnetic field?

Red supergiant stars

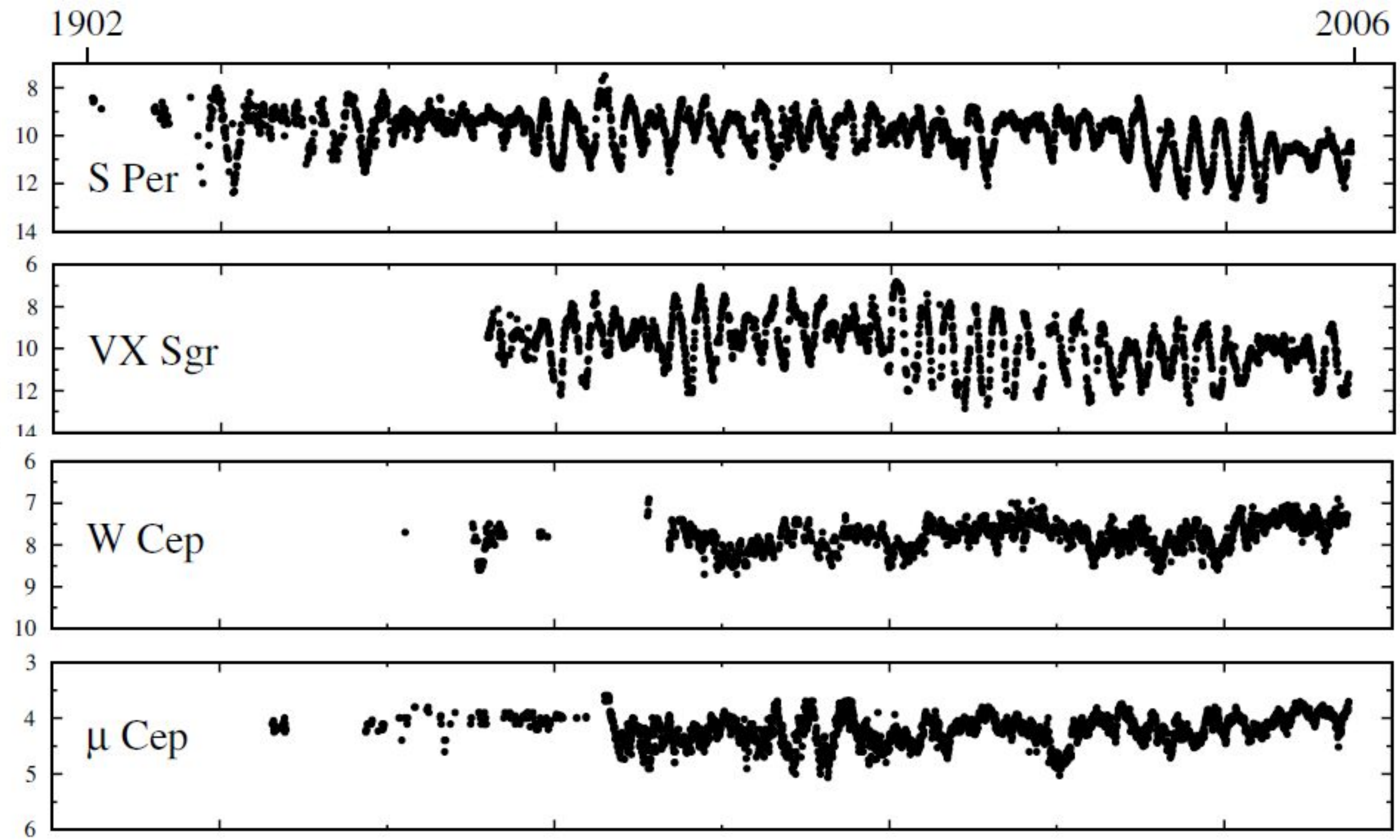

Kiss et al. (2006) ⇒ two photometric periods:

- short (few hundred days) ⇒ convection? pulsations?
- long (few thousand days) ⇒ binarity? magnetic field?

Tomography

μ Cep

- Teff = 3700 K (Levesque 2005)
  3750 K (Josselin & Plez 2007)
- log g = -0.5 (Levesque 2005)
  -0.36 (Josselin & Plez 2007)
- $Mass_{init}$ = 25 M⊙ (Josselin & Plez 2007)
- Radius = 1420 R⊙ (Levesque 2005)
  1258 R⊙ (Josselin & Plez 2007)
- Diameter = 14.11 ± 0.6 mas
  (K band, Perrin et al. 2005)

- **Short photometric period** = 860 d
- **Long photometric period** = 4400 d

Kiss et al. (2006)

3D RHD CO5BOLD (Freytag et al. 2012) simulation "st35gm04n38"

- represents effects of convection
- Teff = 3414 ± 17 K
- log g = -0.39 ± 0.01
- Mass = 5 M⊙
- Radius = 582 ± 5 R⊙
- high-resolution
- the most appropriate simulation

Tomography

- **construction of 1D synthetic spectrum**

-> 1D MARCS (Gustafsson et al. 2008) model atmosphere
-> radiative transfer code TURBOSPECTRUM (Plez 2012)

Tomography

- **construction of 1D synthetic spectrum**

-> 1D MARCS (Gustafsson et al. 2008) model atmosphere (static!)
-> radiative transfer code TURBOSPECTRUM (Plez 2012)

- **computation of the depth of formation of spectral lines**

-> contribution function to the line depression (CFLD) (Albrow & Cottrell, 1996)

$$CF(log(\tau_0)) = \ln(10)\frac{\tau_0}{\kappa_0}\int_0^1 \kappa_l\,(I_c - S_l)\,e^{-\tau/\mu}\,d\mu$$

$$d\tau = \kappa\rho dz$$

Tomography

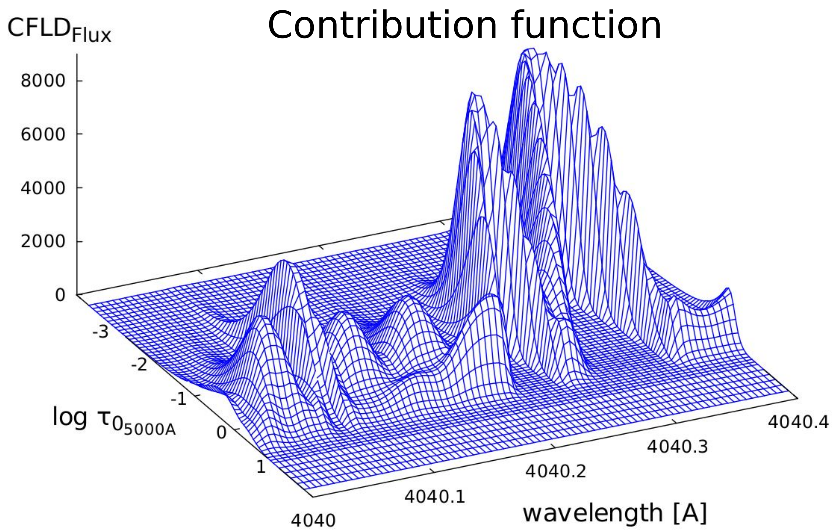

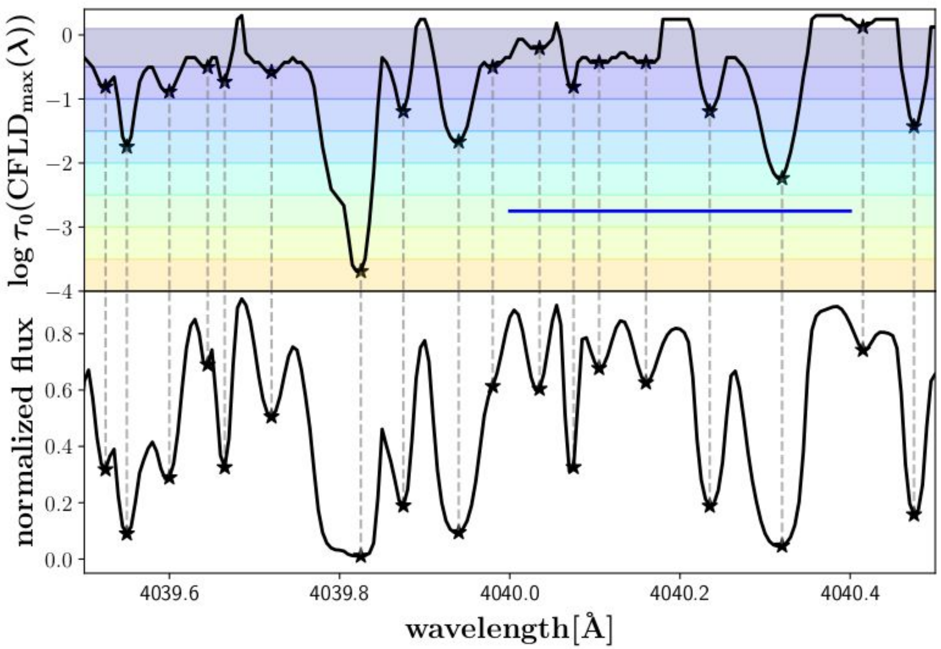

Kravchenko et al. (2018, A&A, 610, A29)

Tomography

- **construction of numerical masks**
  - minima of the depth function
  - keep only atomic lines

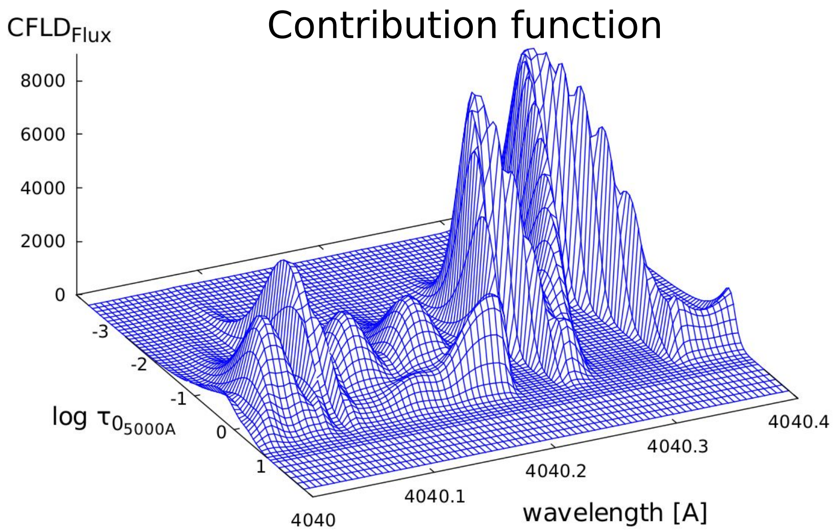

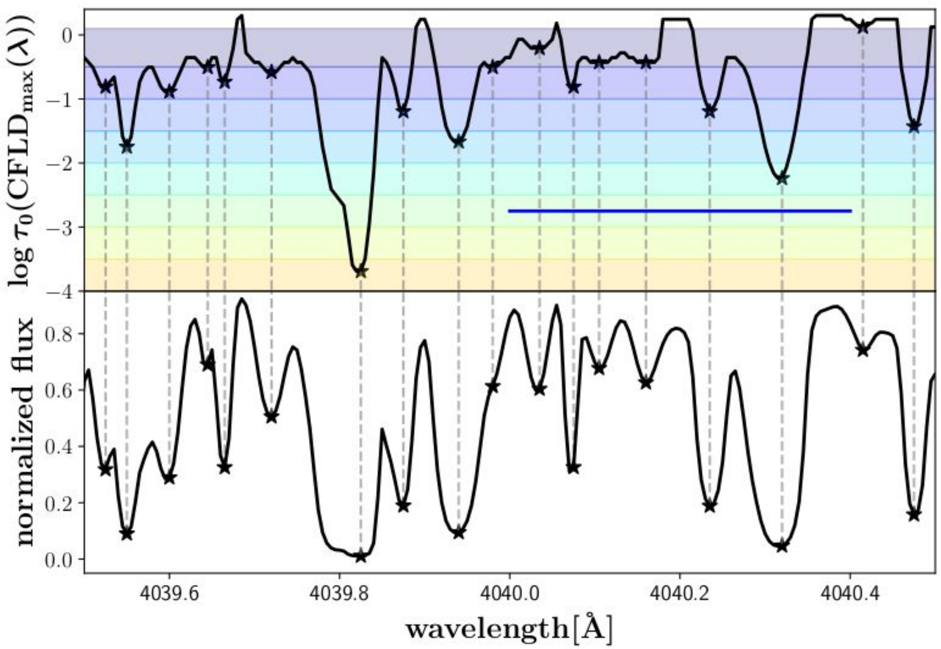

Kravchenko et al. (2018, A&A, 610, A29)

Tomography

- **construction of numerical masks**
  - minima of the depth function
  - keep only atomic lines

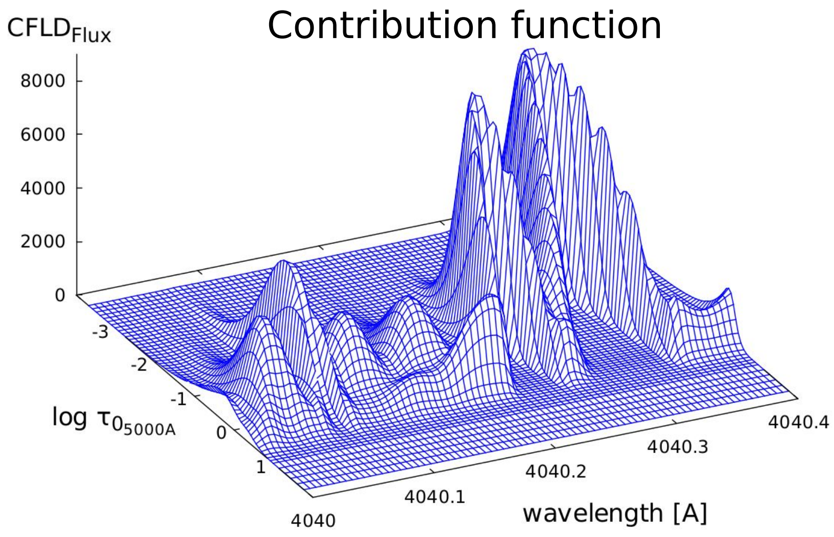

- **cross - correlation of masks with:**
  - observed spectra
  - synthetic spectra

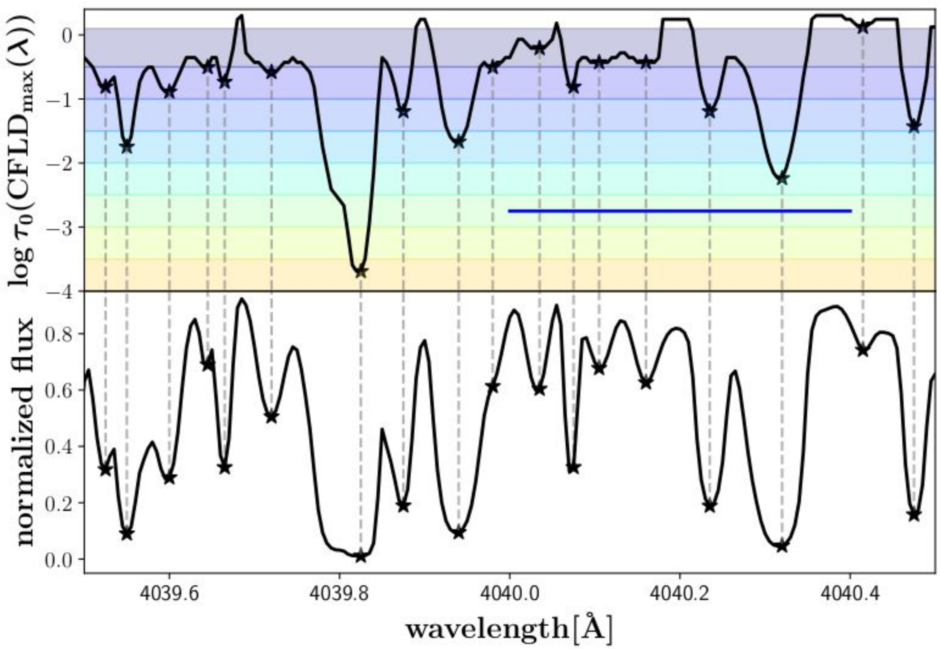

Kravchenko et al. (2018, A&A, 610, A29)

μ Cep: observations

- **HERMES spectrograph (MERCATOR telescope, La Palma, Spain)**
- **Resolution: 85 000**
- **85 high-resolution spectra with S/N ~ 100**
- **time span of 2200 days**

μ Cep: radial velocities

Cross-correlation functions (CCFs)

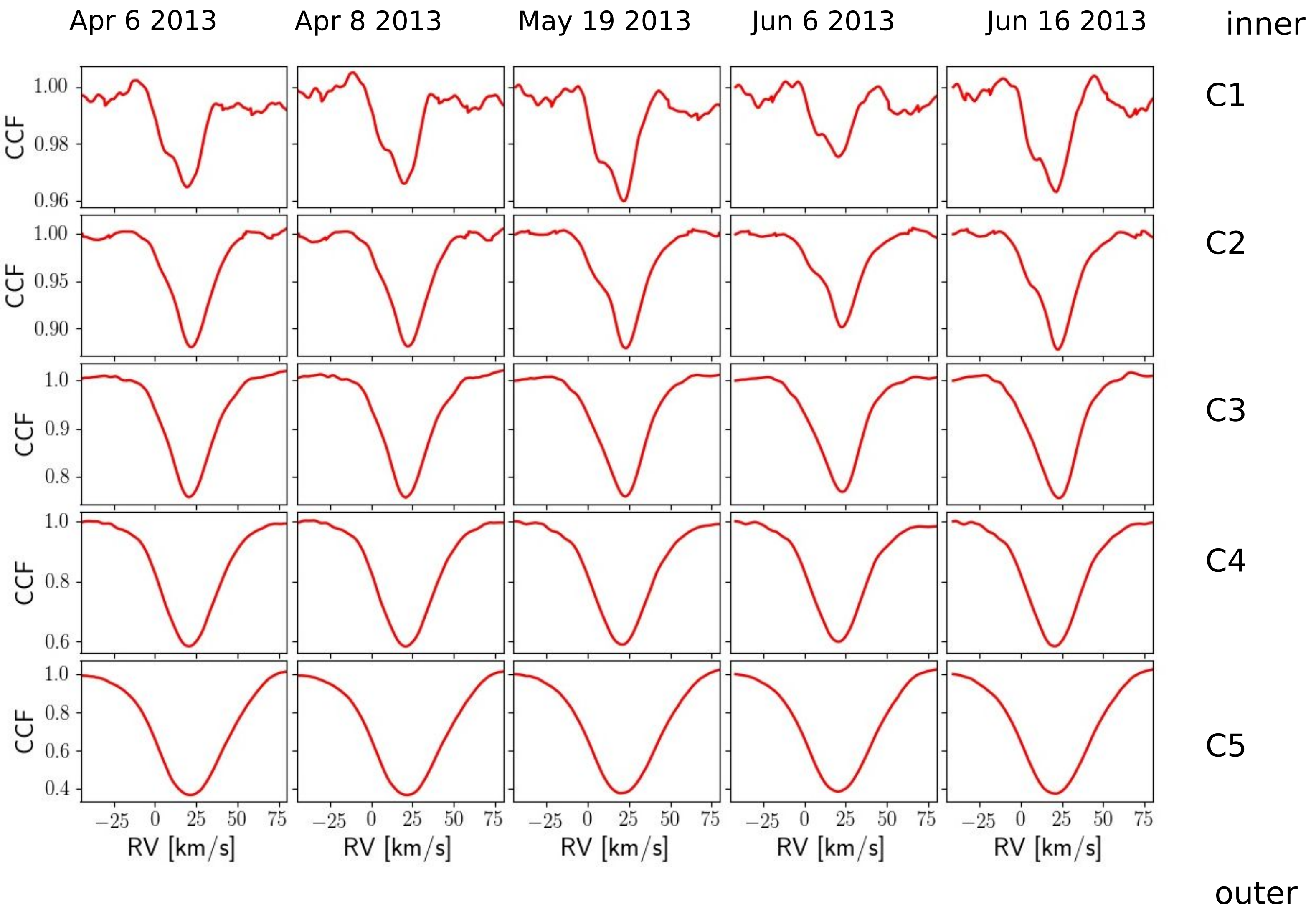

μ Cep: effective temperatures

Computation of the band strength index (Van Eck et al. 2017):

$$B = 1 - \frac{(\lambda_{C,f} - \lambda_{C,i})}{(\lambda_{B,f} - \lambda_{B,i})} \frac{\int_{\lambda_{B,i}}^{\lambda_{B,f}} F_\lambda \mathrm{d}\lambda}{\int_{\lambda_{C,i}}^{\lambda_{C,f}} F_\lambda \mathrm{d}\lambda}$$

Band	$\lambda_{B,i}$	$\lambda_{B,f}$	$\lambda_{C,i}$	$\lambda_{C,f}$
TiO	5847.0	5869.0	5800.0	5847.0
TiO	6159.0	6180.0	6067.0	6119.0
TiO	6187.0	6198.0	6067.0	6119.0
TiO	7054.0	7069.0	7030.0	7050.0
TiO	7125.0	7144.0	7030.0	7050.0

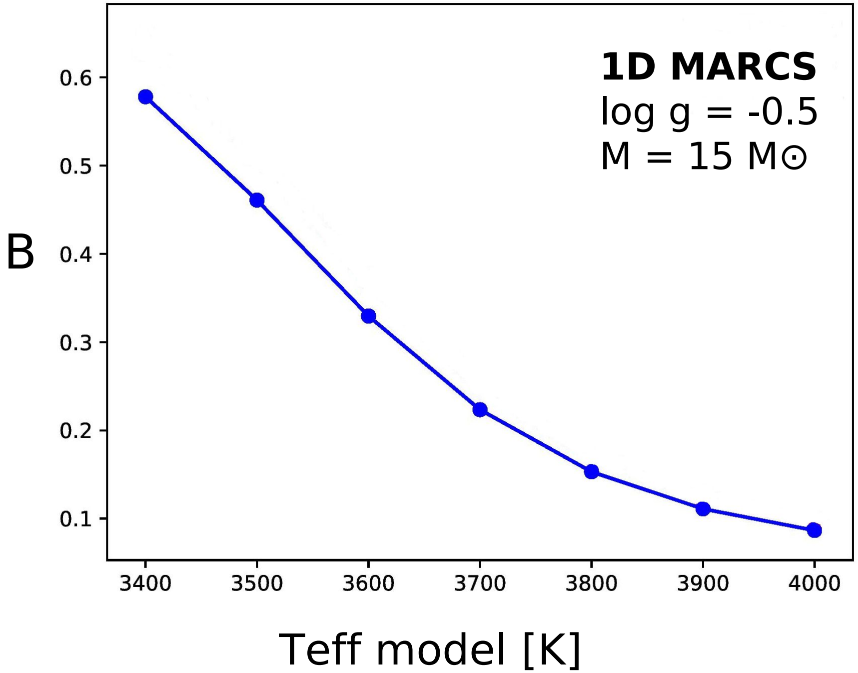

⇒ Teff for μ Cep
(consistent with **3700 K** from *Levesque 2005* and **3750 K** from *Josselin & Plez 2007*)

μ Cep

Phase shift between:

- RV and V magnitude
- RV and Teff

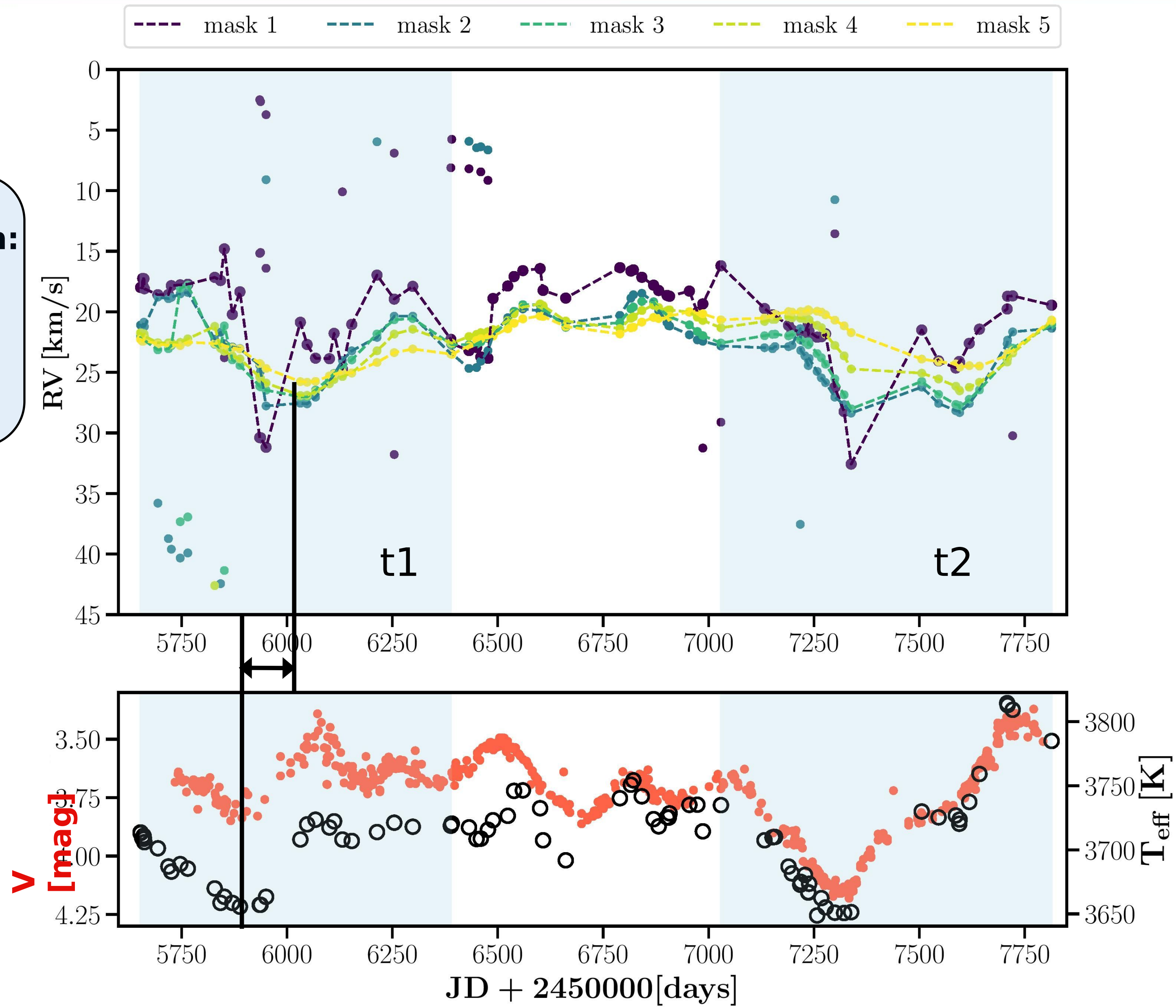

Betelgeuse

Gray (2008): hysteresis loop between T and RV for Betelgeuse ⇒ convection cells

radial velocity (RV)

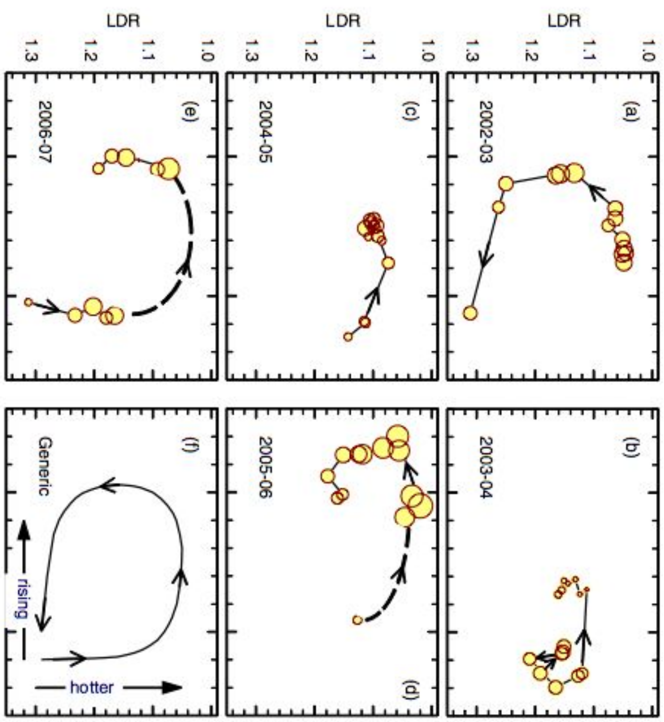

line depth ratio (T indicator)

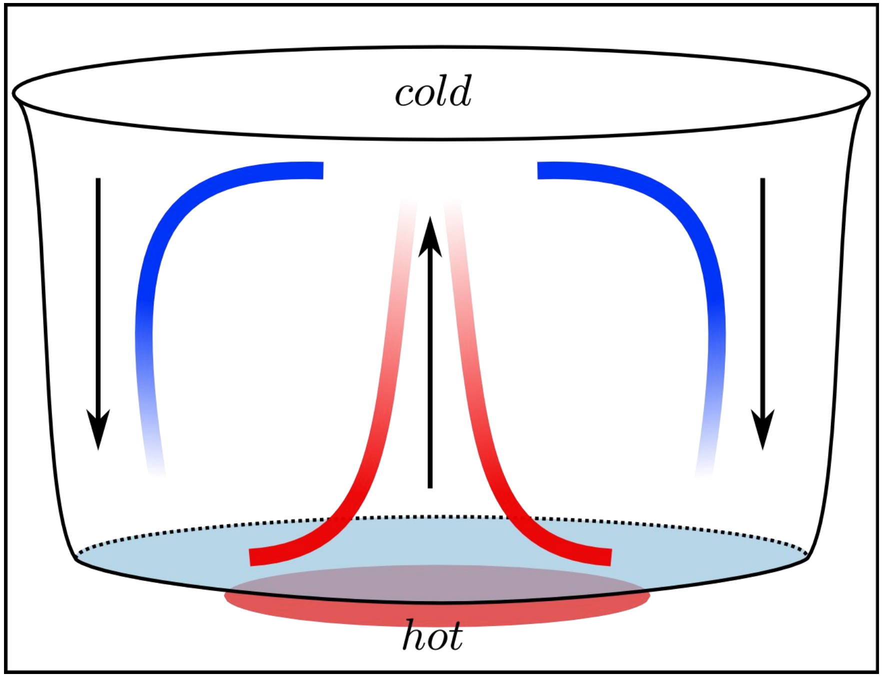

Short photometrical period ~ 400 d (Kiss et al. 2006)

μ Cep

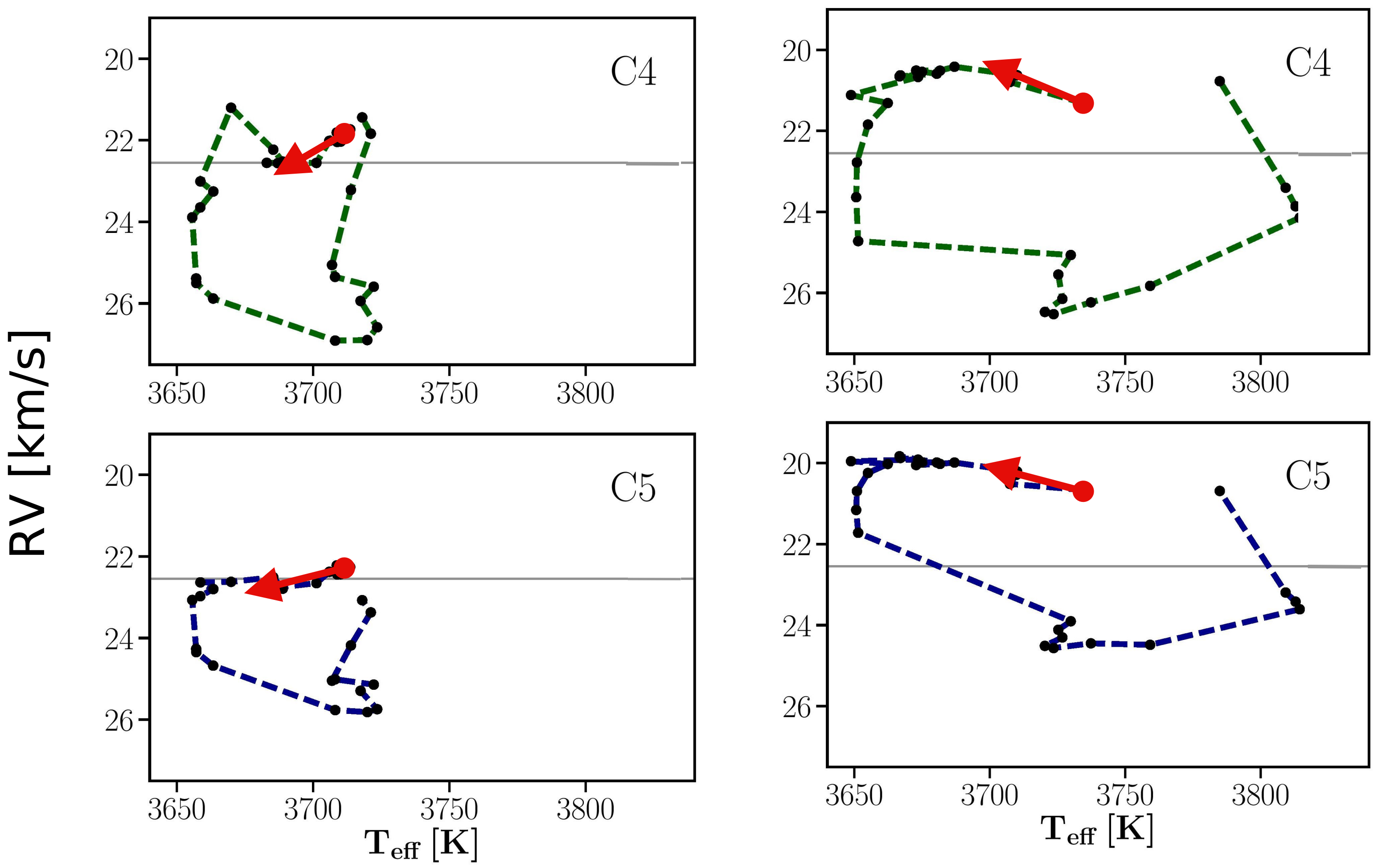

μ Cep

860 days!

t1: 736 days | **t2: 784 days**

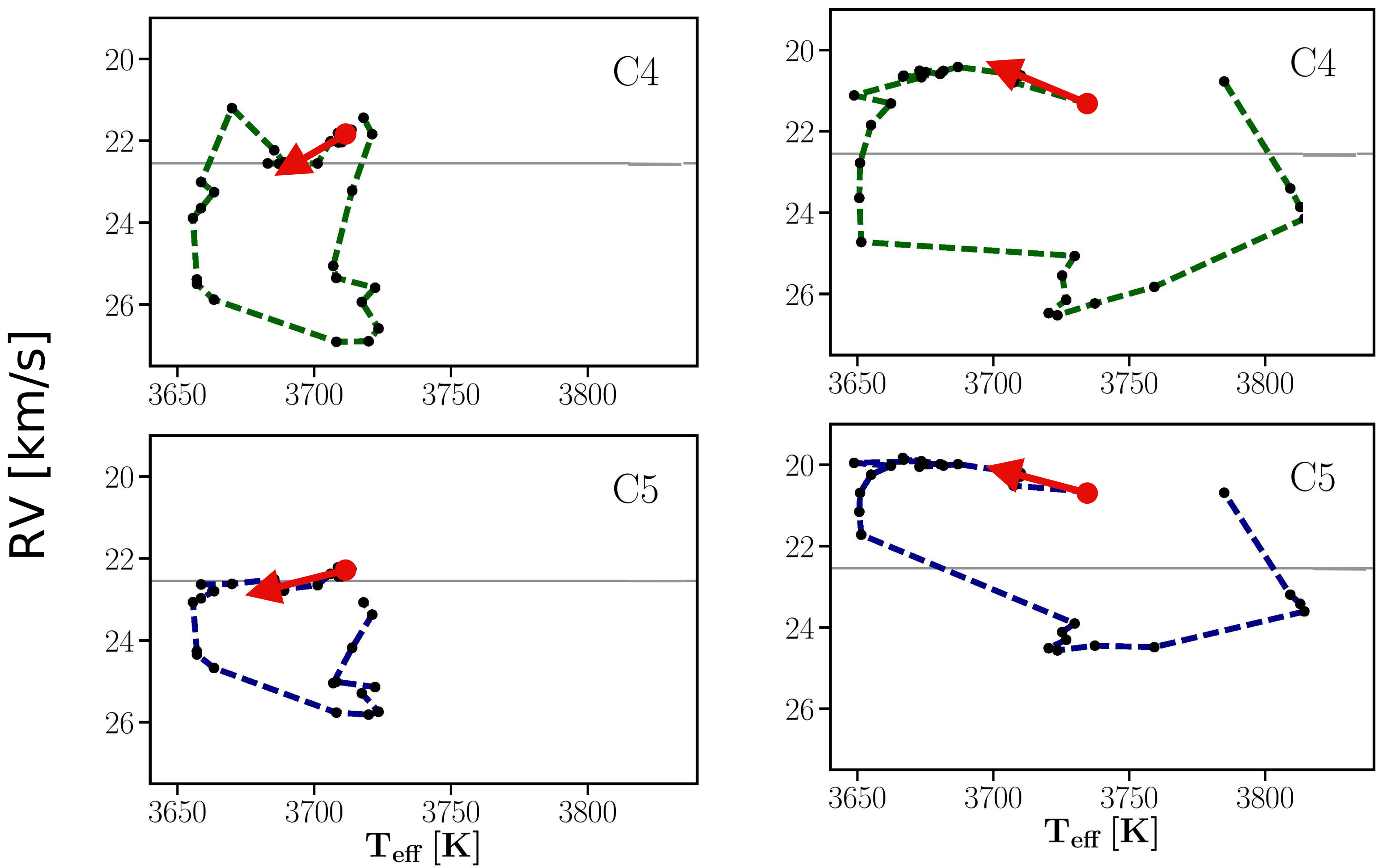

μ Cep

1. Following Gray (2008), hysteresis loop may reveal convection

μ Cep

1. Following Gray (2008), hysteresis loop may reveal convection

2. Convection may be responsible for the short-period photometric variations

3D RHD simulation

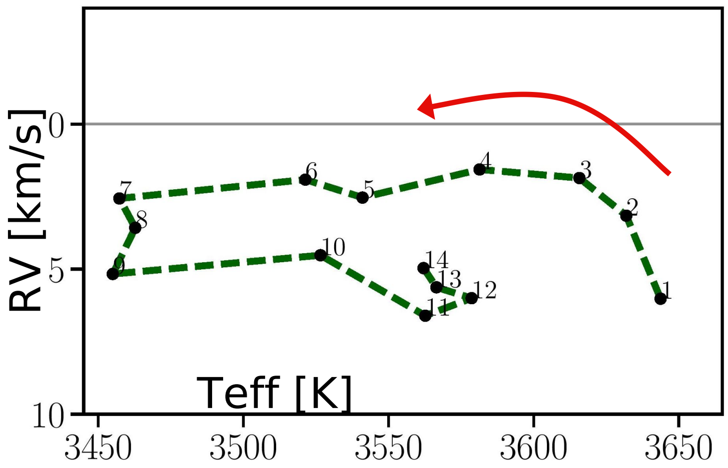

3D RHD simulation: velocity

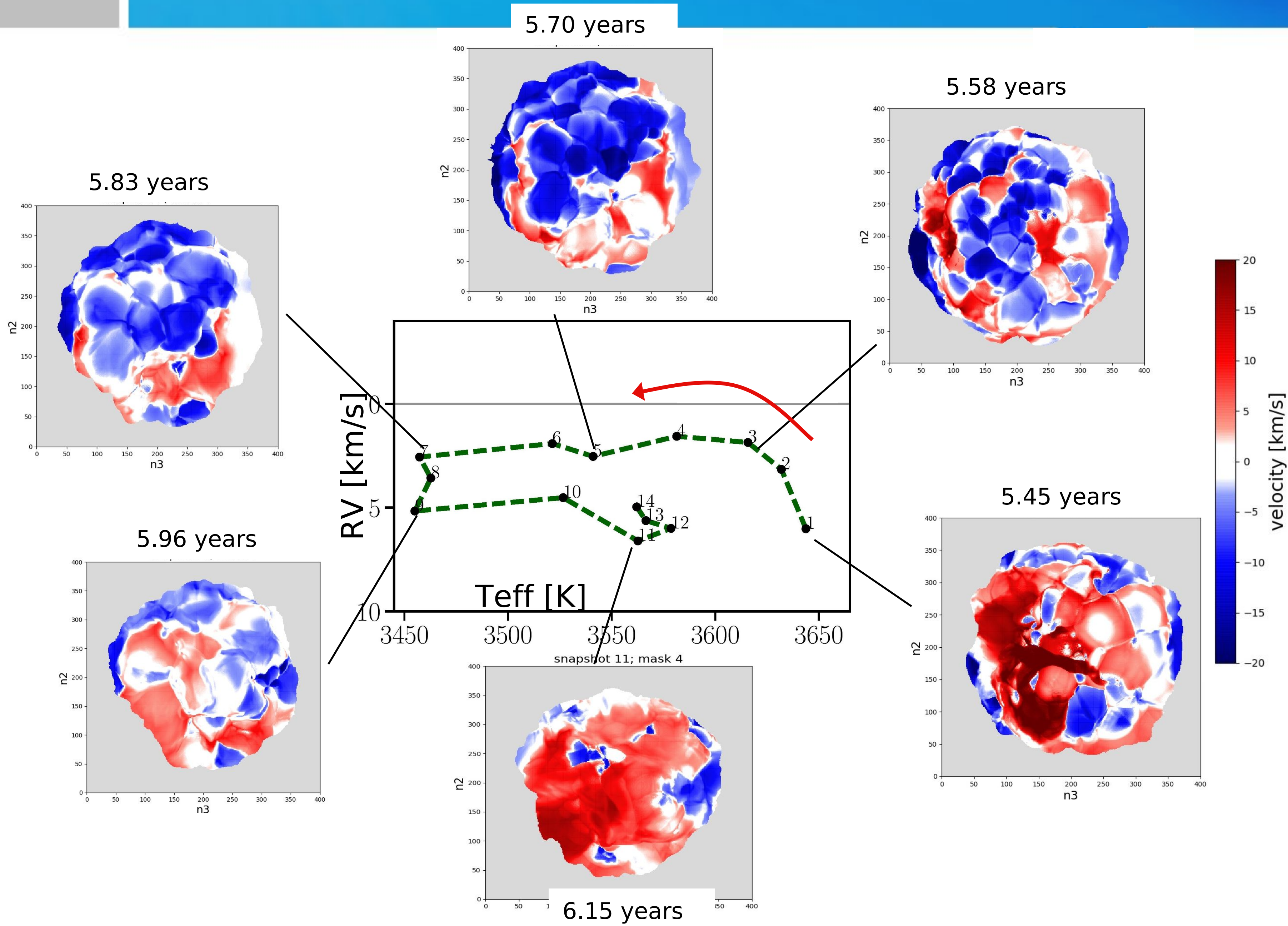

3D RHD simulation: temperature

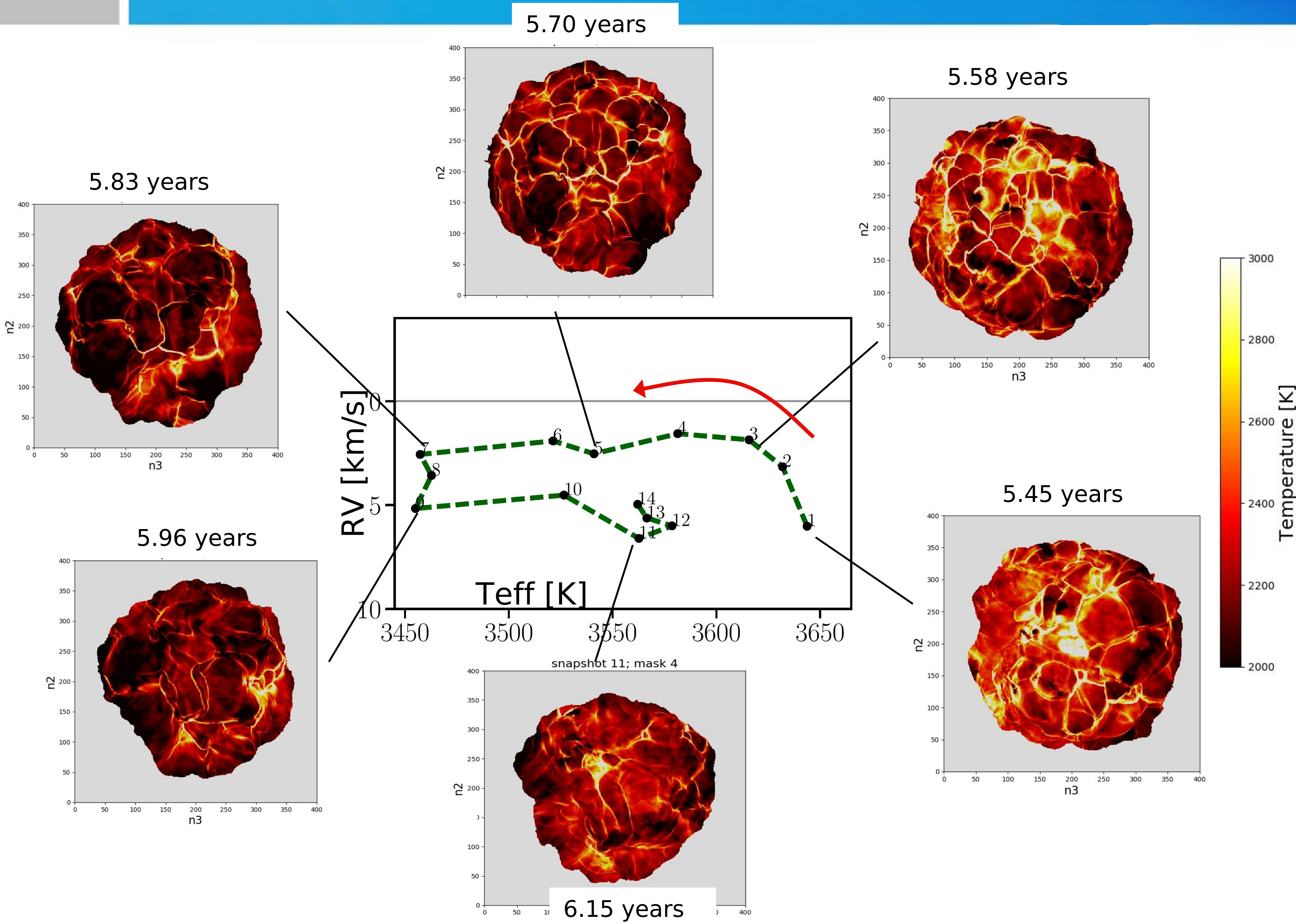

Observations vs 3D simulation

	Observations: µ Cep		**3D simulation**
	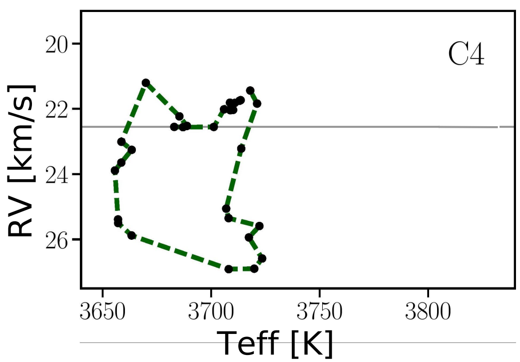	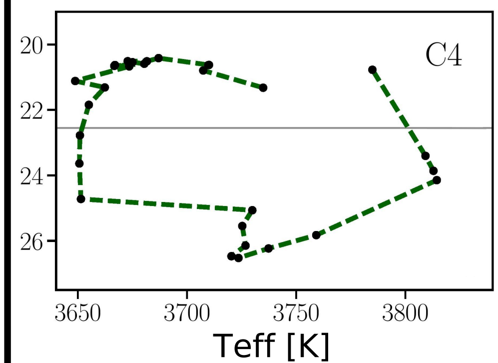	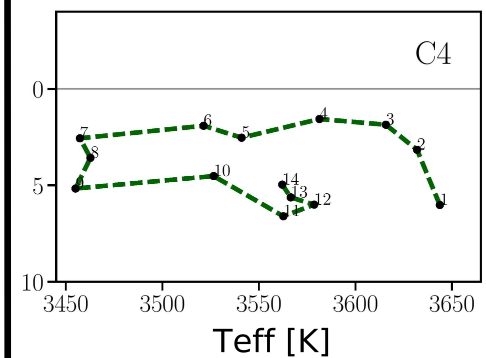
RV extent	6 km/s	7 km/s	5 km/s
T extent	70 K	200 K	200 K
Timescale	736 d	784 d	400 d

Observations vs 3D simulation

Betelgeuse Gray(2008)	**Observations: μ Cep**		**3D simulation**
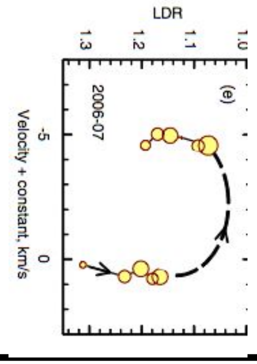	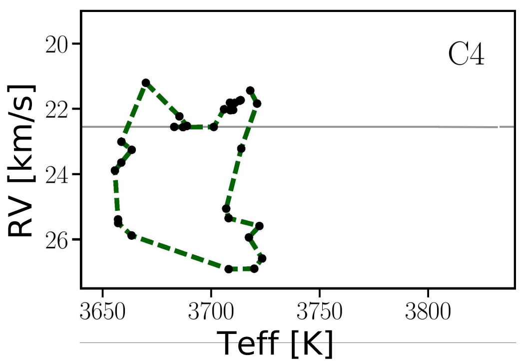	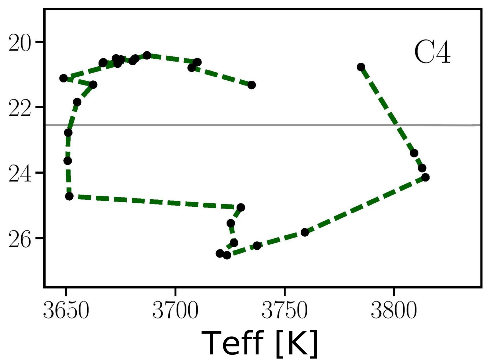	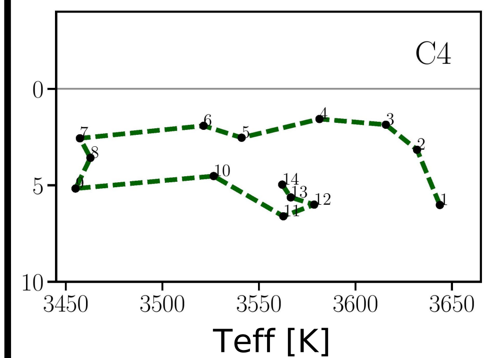
6 km/s	6 km/s	7 km/s	5 km/s
>100 K	70 K	200 K	200 K
~ 400 d	736 d	784 d	400 d

- **similar qualitative behavior**
- **pointing at convection which may be responsible for the photometric variations**

Conclusions

The tomographic method was applied to:

1. a large sample of the high-resolution spectra of μ Cep

2. snapshots from the 3D RHD simulation

⇒ behavior in the temperature-velocity plane is very similar

Short-period photometric variations can probably be accounted for by convection.

work in progress……

NEXT STEPS: Application of the tomographic method to time-series of high-resolution spectra of a sample of RSG stars

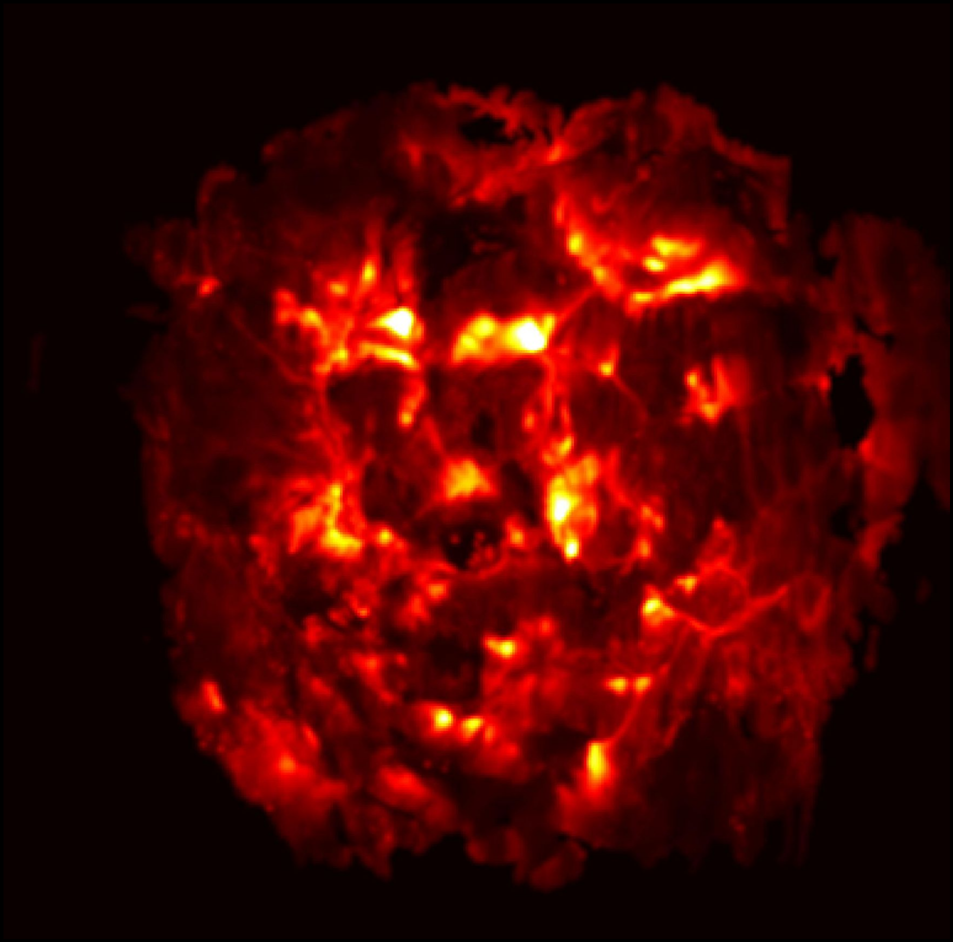

Thank you!

Scaling relations: test

$\log(x_{Tremblay}) = 1.75 \log[T_{eff} - 300 \log(g)] - \log(g) + 0.05[Fe/H] - 1.87$

$\log(x_{Trampedach}) = (1.321 \pm 0.004) \log(T_{eff}) - (1.0970 \pm 0.0003) \log(g) + (0.031 \pm 0.036)$

$\log(x_{Freytag}) = \log(T_{eff}) - \log(g) - \log(\mu) + 0.92$; $\mu = 1.3$ g mol^{-1}

$t_{decay,Tremblay} = 2.08\, g^{-1} (T_{eff} - 300 \log(g))^{1.75}\, 10^{0.05[Fe/H]} \quad \Rightarrow \quad t = 2\pi\, t_{decay,Tremblay}$

Tremblay et al. (2013), Trampedach et al. (2013), Freytag et al. (1997)

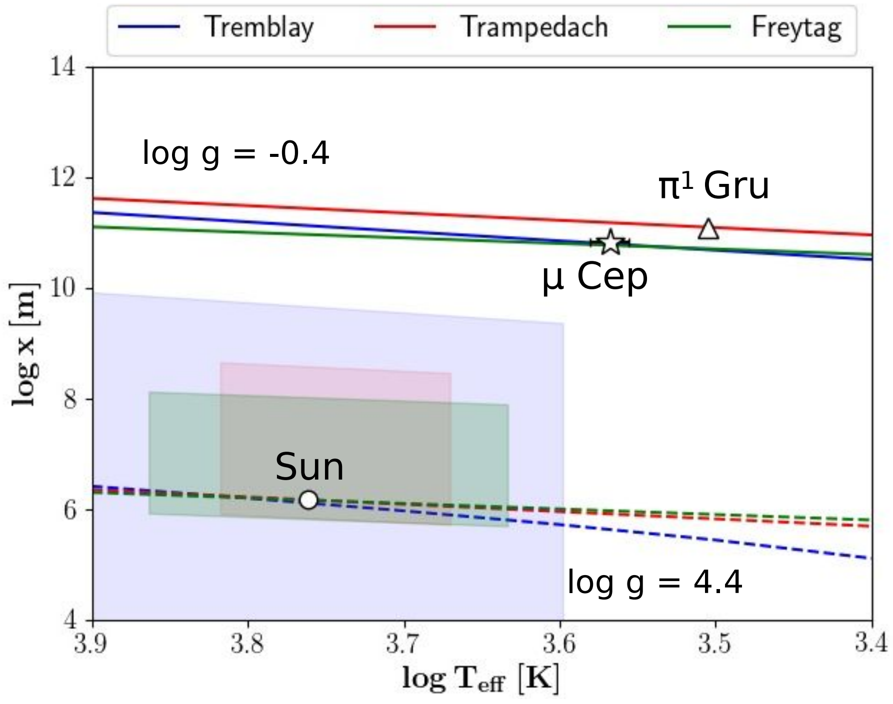

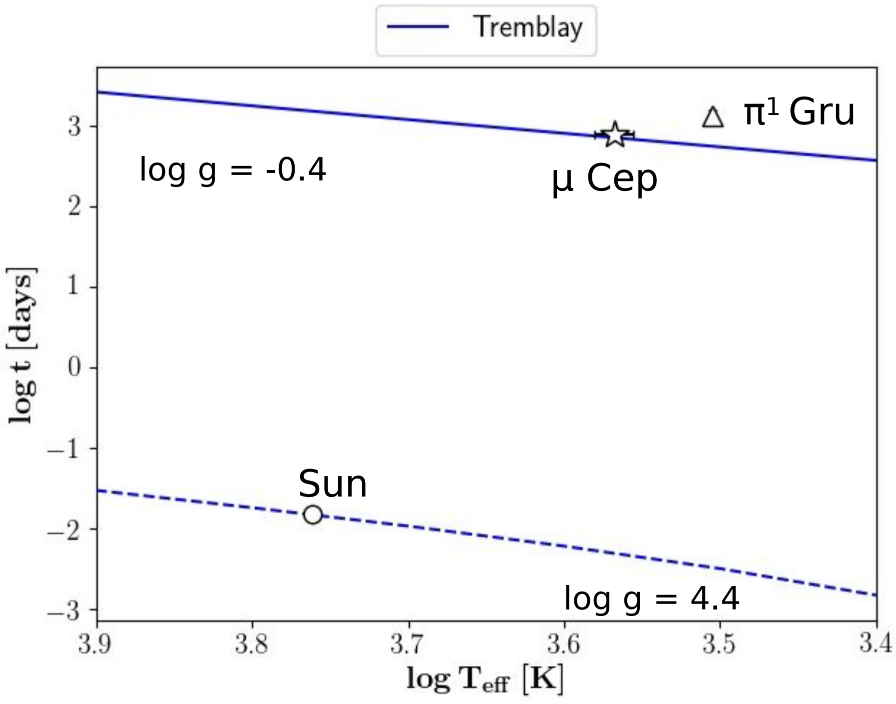

π¹ Gru: Paladini et al. (2018), *Nature*

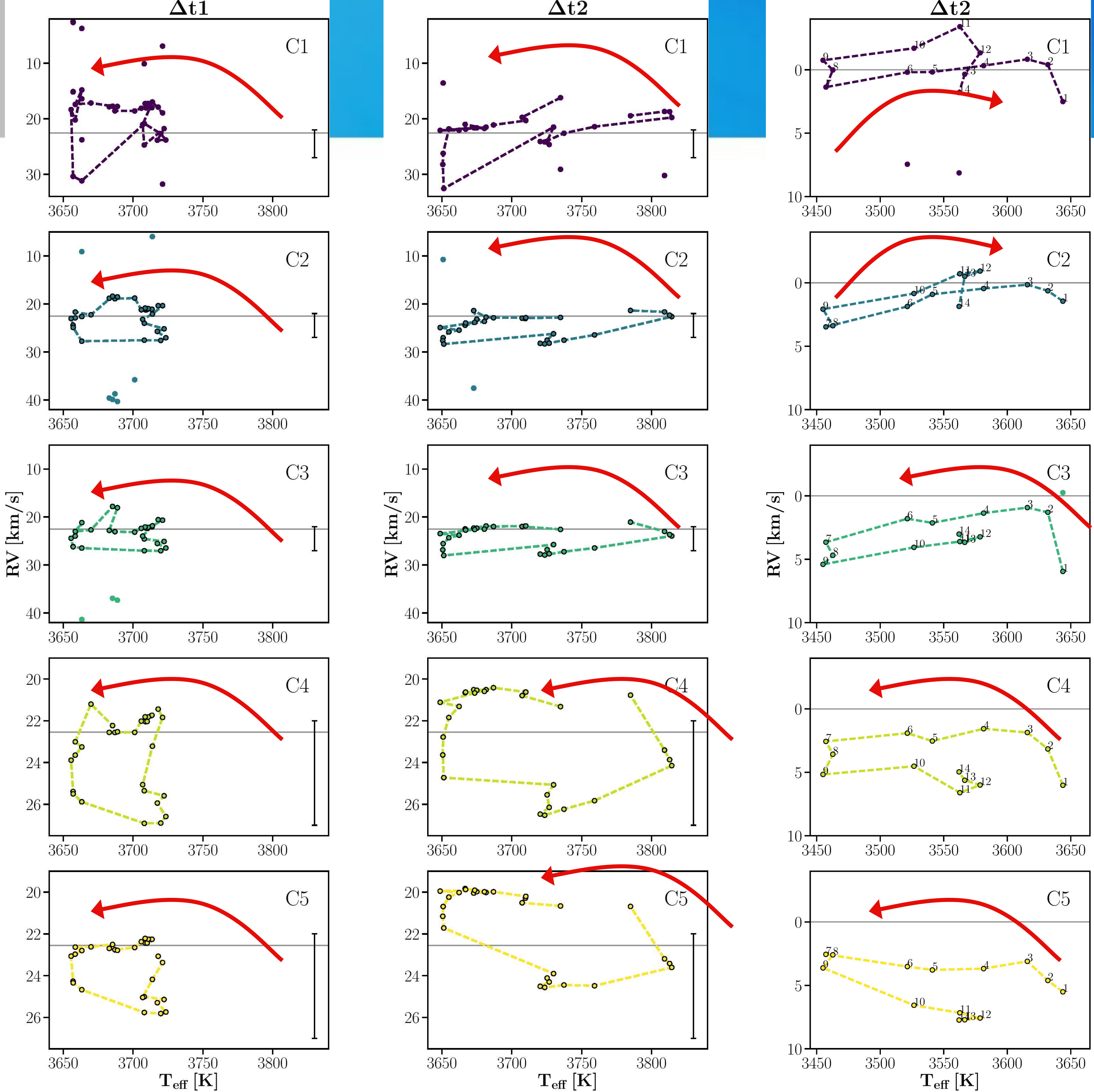

Δt1
Δt2
Δt2
C1
C2
C3
C4
C5
RV [km/s]
T_{eff} [K]

3D RHD simulation: velocity

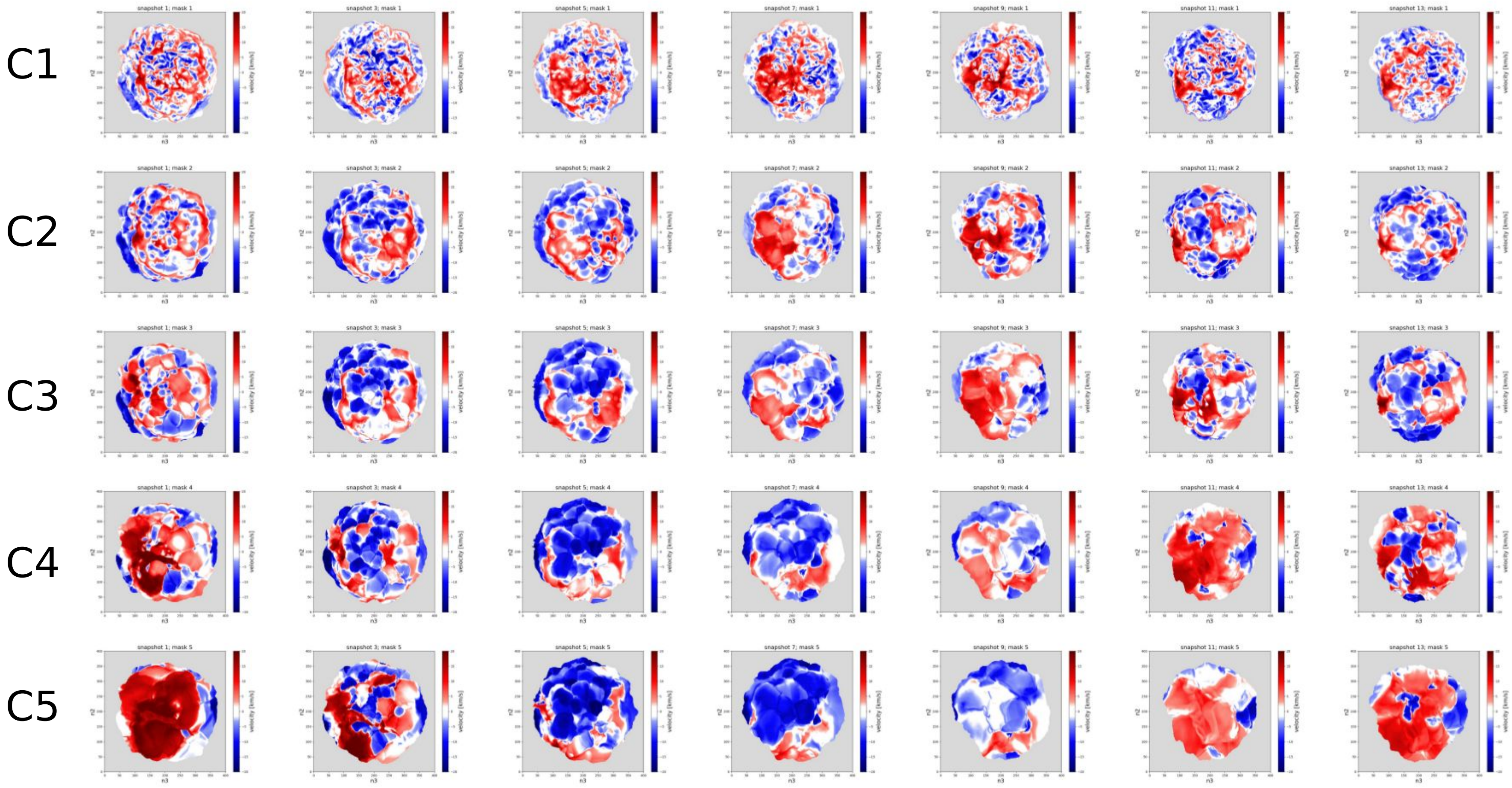

Kravchenko et al. (in prep)

Tomography

Table 2. Properties of the tomographic masks.

Mask	$\log \tau_0$ limits*	number of lines
C1	$-1.0 < \log \tau_0 < 0.5$	419
C2	$-2.0 < \log \tau_0 < -1.0$	1750
C3	$-3.0 < \log \tau_0 < -2.0$	1199
C4	$-4.0 < \log \tau_0 < -3.0$	433
C5	$-5.0 < \log \tau_0 < -4.0$	378

* τ_0 is the reference optical depth computed at $\lambda =$ 5000Å.

Kravchenko et al. (in prep)

Tomography

Can tomography correctly recover the velocity field?

- cross-correlation functions (CCFs) computed from the synthetic snapshot spectrum

- velocity distribution from the same snapshot (green histograms)

➪ **Good agreement**

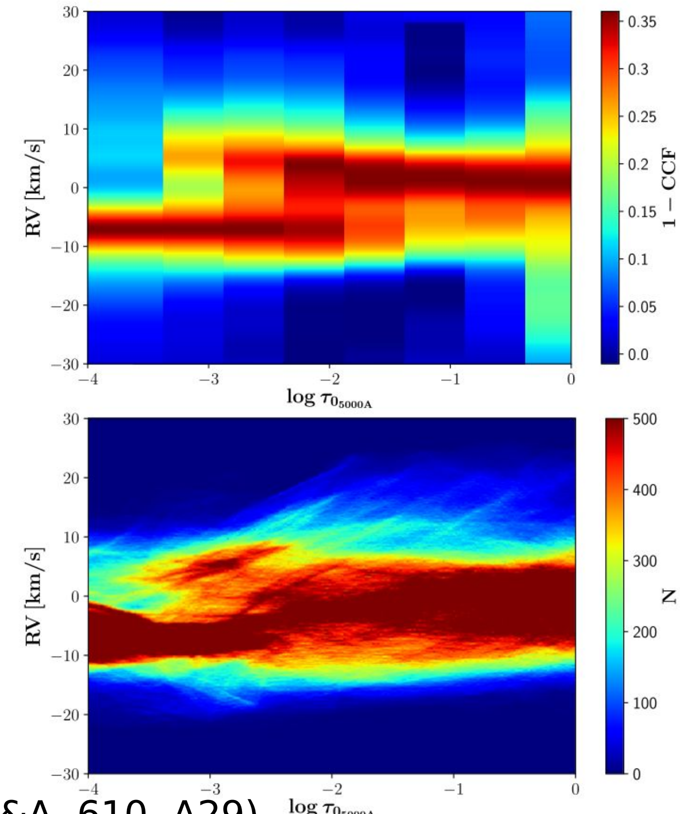

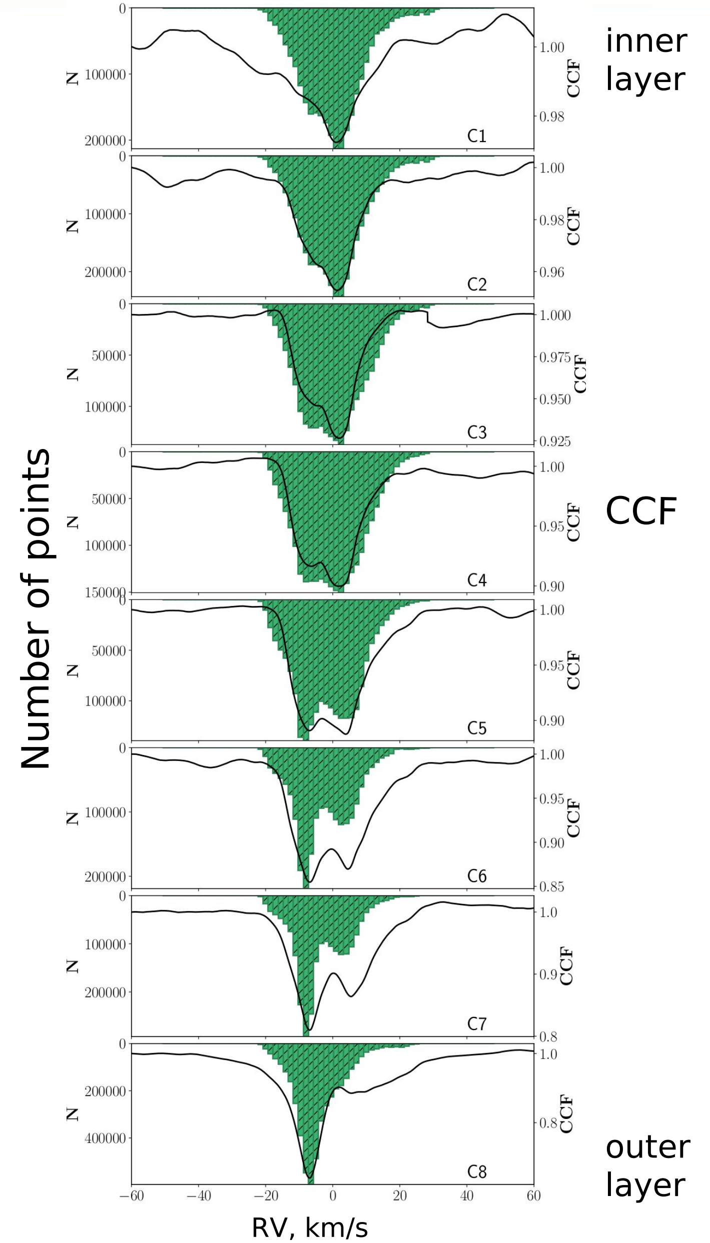

Kravchenko et al. (2018, A&A, 610, A29)

3D RHD simulation

- st35gm04n38
- 401^3 grid points
- Teff = 3414 ± 17 K
- log g = -0.39 ± 0.01
- Mass = 5 M⊙
- Radius = 582 ± 5 R⊙

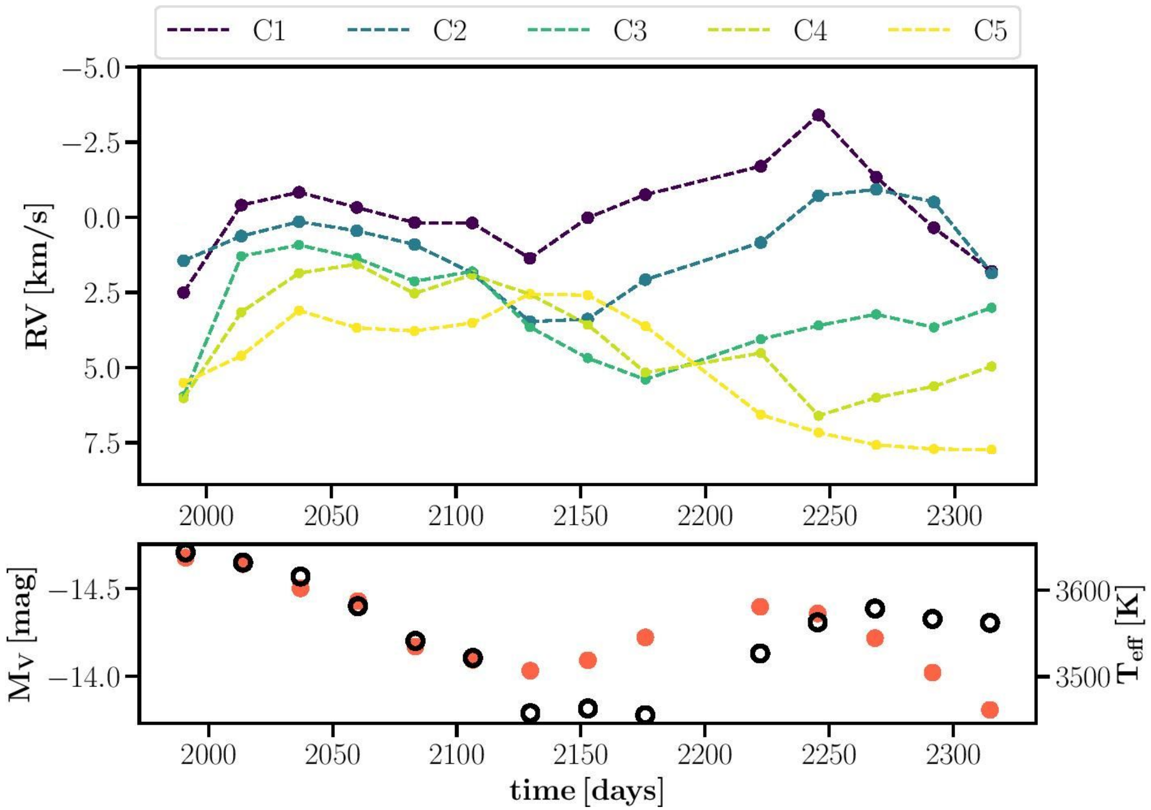

μ Cep

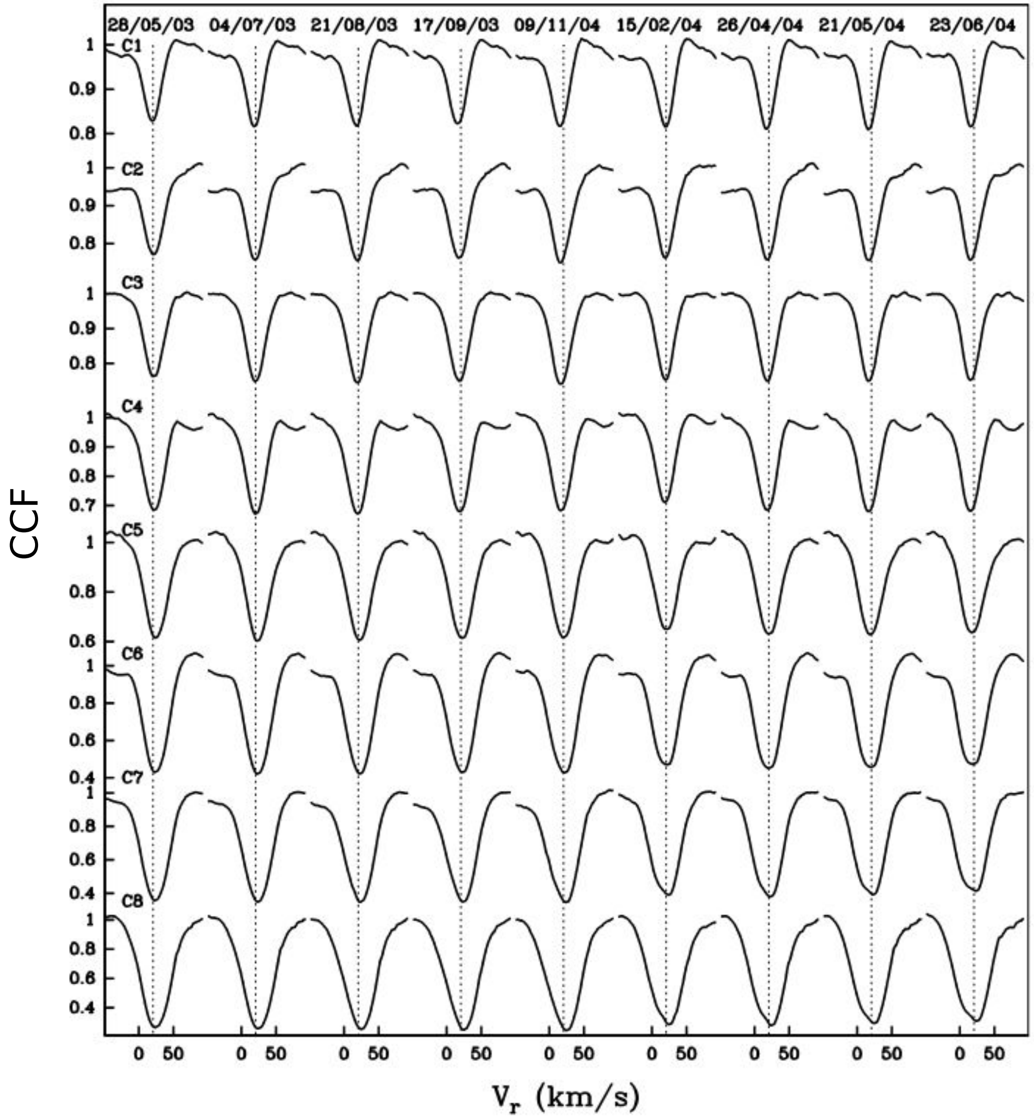

Josselin & Plez (2007) → no line doubling

μ Cep

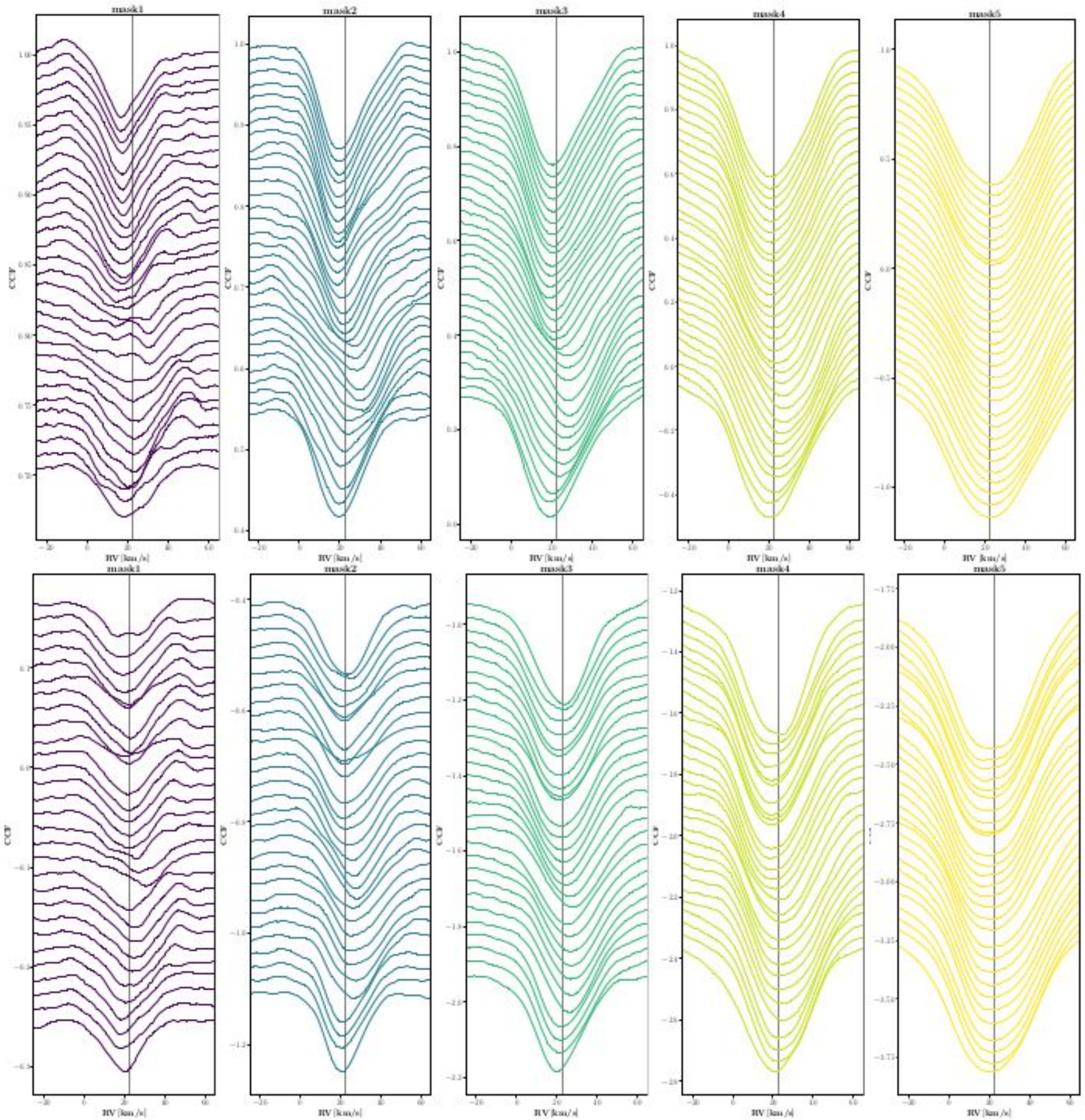

Fig. 14. *From top to bottom:* CCFs corresponding to the time range Δt1 and Δt2 (see Fig. 11). *From left to right:* Different masks, C1 probes the innermost atmospheric layer, C5 - the outermost. Vertical lines in all panels indicate the mean radial velocity in all masks.

Kravchenko et al. (in prep)

μ Cep

M_{bol} = -8.88 from Josselin & Plez (2007)

Evolutionary tracks from Eckström et al. (2012)

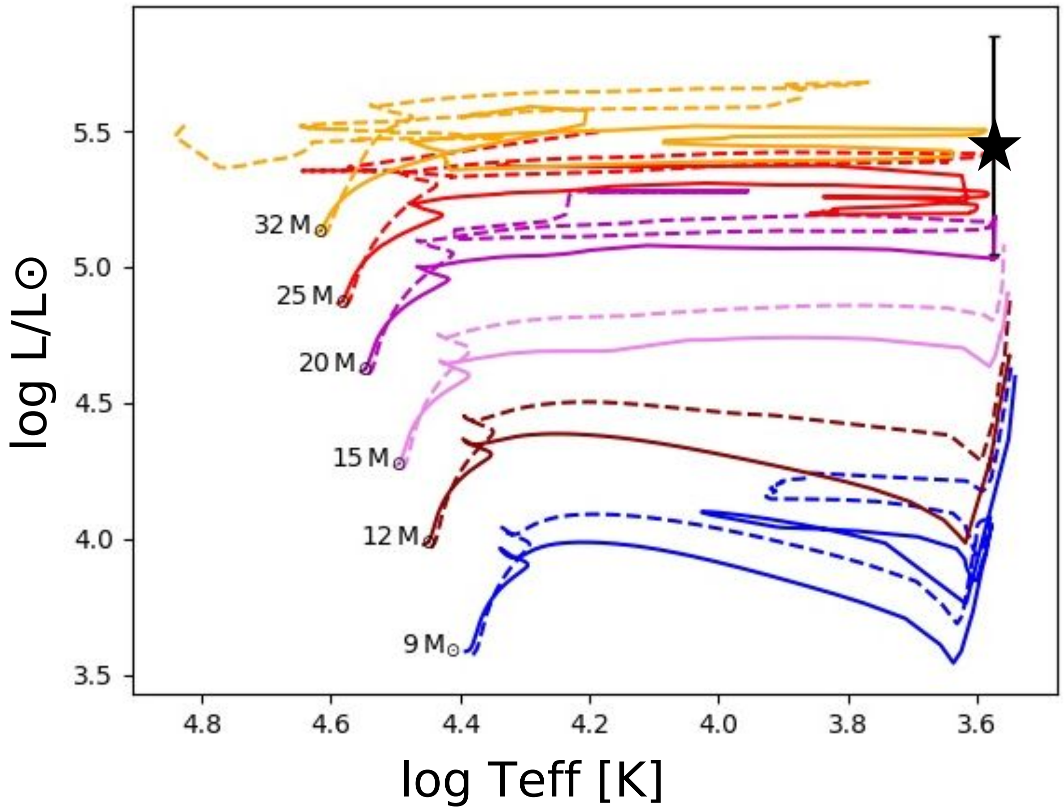

Kravchenko et al. (in prep)

Tomography

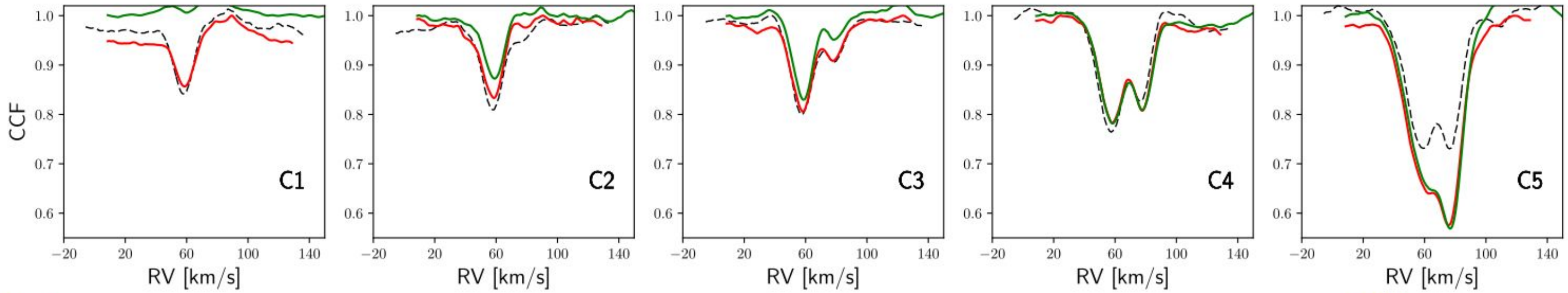

Fig. 5. Black dashed line: sequence of CCFs obtained from a V Tau spectrum (JD 2451093.5) using masks of Alvarez et al. (2001a; their Fig. 18). Red line: the CCF profiles obtained from the same spectrum using masks with identical log τ limits but built using maxima of the CFLD, as described in Sect. 2.2. Green line: CCF profiles obtained from the same spectrum using masks built from Eq. (4) in Sect. 2.4.

Kravchenko et al. (2018, A&A, 610, A29)

Tomography

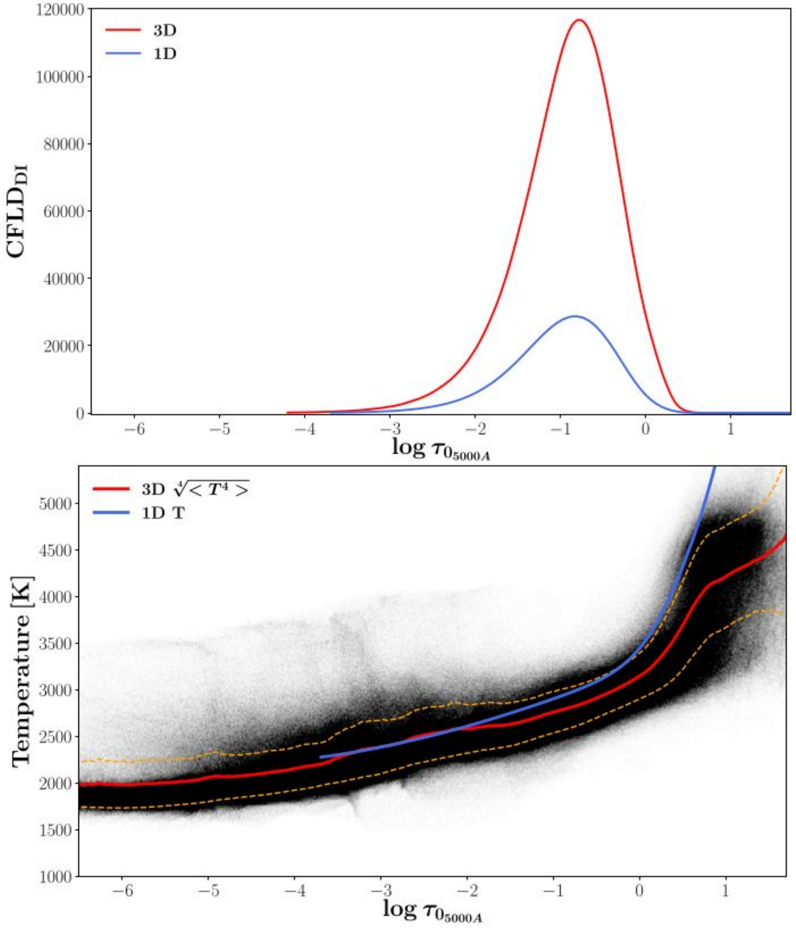

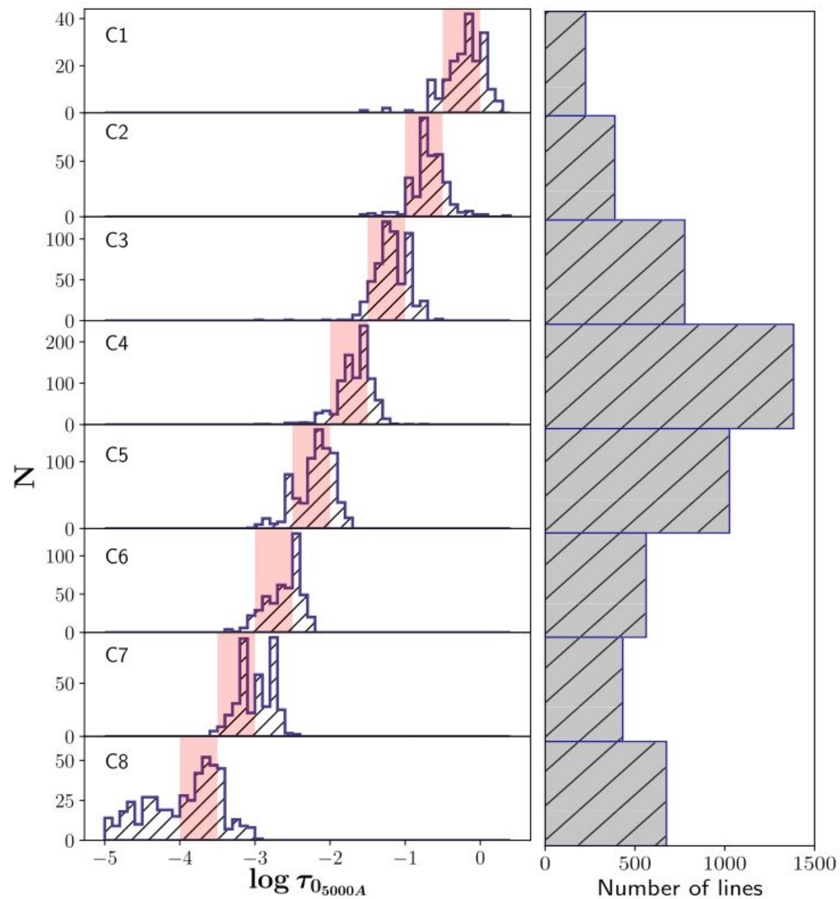

Kravchenko et al. (2018, A&A, 610, A29)

Tomography

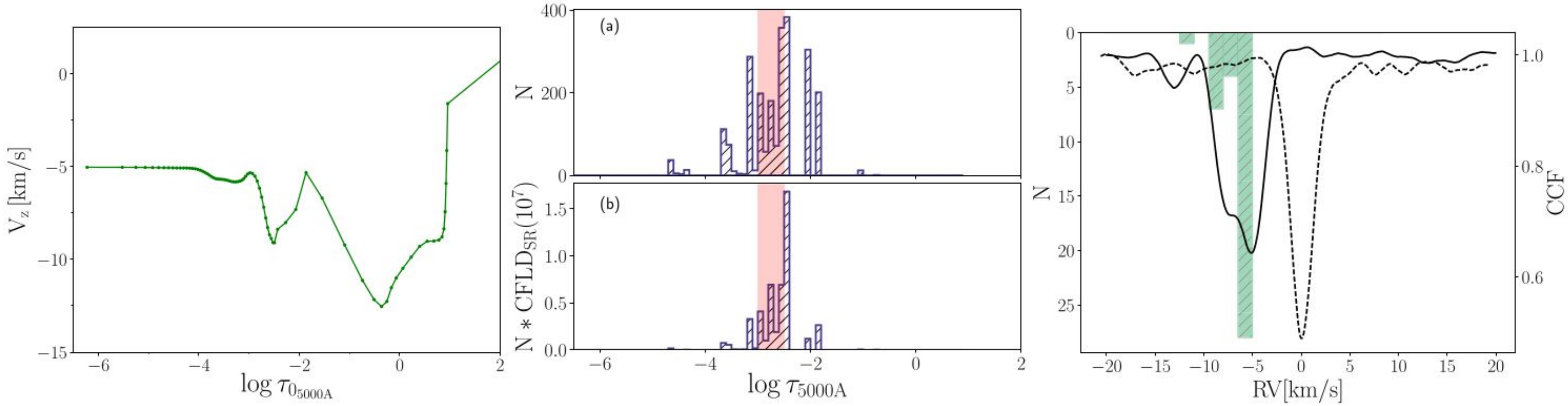

Fig. 14. *Left panel*: V_z as a function of the reference optical depth for the ray 1 of the 3D simulation. *Middle panel*: distribution of formation depths of lines contributing to the mask C6 for the ray 1 weighted (*b*) and not weighted (*a*) by the CFLD. *Right panel*: CCF obtained by cross-correlation of the synthetic spectrum [*with* (black solid line) and *without* (black dashed line) including the velocity field in the 3D simulation] for the ray 1 of the 3D snapshot with the mask C6. Green bars show the distribution of velocities corresponding to formation depths of lines contributing to the mask C6.

Kravchenko et al. (2018, A&A, 610, A29)

Schwarzschild scenario

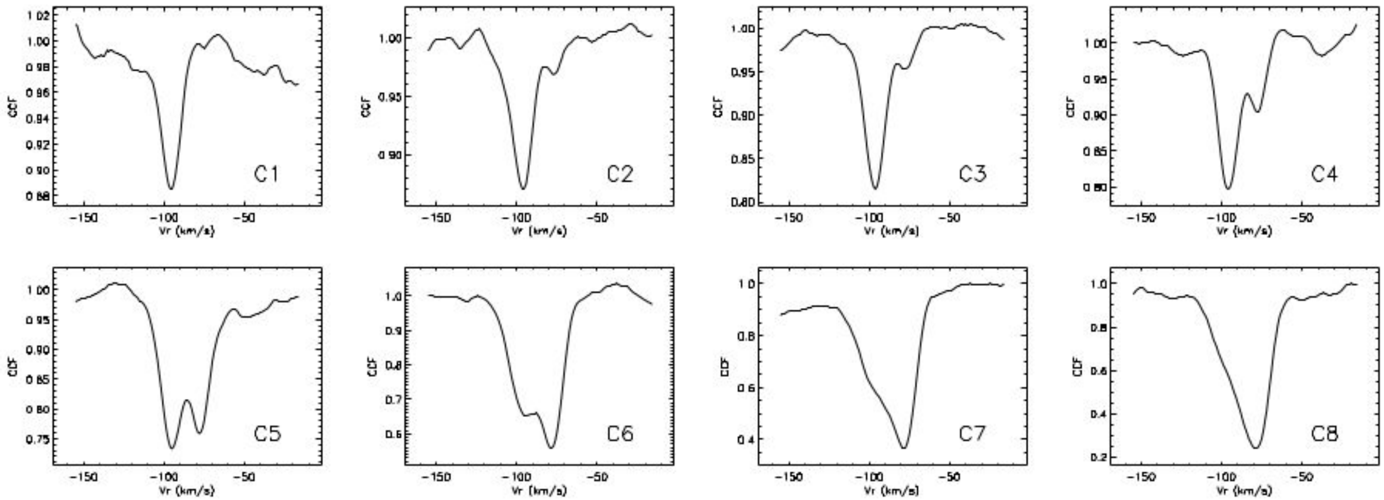

Fig. 3 The CCFs of the Mira Z Oph at phase 0.08 (1998, August 05-06) obtained with the tomographic masks. The set of tomographic masks used for Z Oph was constructed from a synthetic spectrum at $T_{\rm eff} = 3500$ K and $\log g = 0.9$ (see [3] for details). Note how the shape of the CCFs evolve from the innermost layer (involving ascending matter only, hence C1 exhibits a single blue peak) to the outermost layer (involving mostly matter falling in, hence C8 exibits predominantly a red peak). This spatial sequence of line doubling reflects the presence of a shock wave in the line-forming region, with the shock front being centered on the layer probed by the mask C5.

Jorissen et al. (2015)